Light-scattering characterization of spherical particles prepared by the dispersion polymerization of methyl methacrylate in a non-aqueous medium*

Jaroslav Stejskal, Pavel Kratochvíl, Petr Koubík, Zdeněk Tuzar and Josef Urban
Institute of Macromolecular Chemistry, Czechoslovak Academy of Sciences, 162 06 Prague 6, Czechoslovakia

Martin Helmstedt
Karl-Marx Universität, Sektion Physik, Linnéstrasse 5, 7010 Leipzig, GDR

and Aubrey D. Jenkins
The School of Chemistry and Molecular Sciences, The University of Sussex, Brighton BN1 9QJ, UK
(Received 15 November 1989; revised 19 January 1990; accepted 6 February 1990)

Poly(methyl methacrylate) particles stabilized by polystyrene-*block*-poly(ethylene-*co*-propylene) in decane were prepared by dispersion polymerization. Scanning electron microscopy showed that the particles are spherical, relatively uniform in size and of submicrometre dimensions. Particle molar masses M_w of the order of magnitude 10^9 g mol^{-1} and radii of gyration can be determined with good accuracy by static light scattering if a logarithmic version of the Zimm plot is used. Geometric dimensions were calculated from the radii of gyration. Information on particle swelling can also be derived from the light-scattering data. The particle cores are found to be considerably swollen. The dimensions obtained from static light scattering are in accord with the dynamic light-scattering data.

(Keywords: dispersion polymerization; poly(methyl methacrylate) dispersion; block copolymer; light scattering; particle molar mass; particle size)

INTRODUCTION

The practical applicability of static light scattering[1] (SLS) for the determination of molar mass is limited to particles with size smaller than the wavelength of incident light, i.e. with dimensions of a few hundred nanometres. For highly swollen polymer coils, this corresponds to molar masses of the order of magnitude 10^6 to 10^7 g mol^{-1}. When the dimensions of the scattering particles become larger, the angular dependences of scattered light become curved, and extrapolation to zero angle of observation is ambiguous or imprecise. Nevertheless, even particles of high molar mass can be characterized by light scattering without difficulties if they are substantially more compact than polymer coils and, consequently, relatively small. This is especially true for aggregates of macromolecules, such as block and graft copolymer micelles. Micellar molar masses of the order of magnitude 10^7 g mol^{-1} were reported for micelles of block copolymers in solvents selective for blocks of one type[2,3]. Still higher molar masses of the order of 10^8 g mol^{-1} were found for polymer particles in aqueous media: poly(methyl methacrylate) (PMMA) dispersions stabilized by grafted gelatin[4], poly(methyl acrylate–acrylic acid) lattices[5], or native glycogen[6].

Recently, dispersion polymerization has been studied intensively[7,8]. This type of polymerization resembles precipitation polymerization since the resulting polymer is insoluble in the reaction medium, but, in contrast to emulsion or suspension polymerization, the monomer is completely miscible with the diluent. Macroscopic precipitation of the polymer is prevented by the presence of a steric stabilizer. Block[9] or graft[10] copolymers can be used for this purpose. For effective stabilization, blocks of one type must be insoluble in the reaction medium (the anchor blocks, *Figure 1*). Blocks of the other type must be soluble, and they create the shell (corona) of the dispersion particle. Virtually uniform particles within the range of diameter 0.1–10 μm can be prepared by this type of polymerization[7,8].

So far, the dimensions of the dispersion particles have been characterized mainly by electron microscopy[7,8]. The light-scattering technique, in both the static and dynamic modes, is a powerful tool for the investigation of the dispersion particles, especially in the submicrometre range. Static light scattering provides the absolute value of molar mass of the particles and their radius of gyration. Dynamic light scattering yields the hydrodynamic radius of the particles. Additional information is obtained by combining the data. In the present paper, this is illustrated with reference to PMMA dispersions stabilized by polystyrene-*block*-poly(ethylene-*co*-propylene) copolymer

* Dedicated to Professor Walther Burchard on the occasion of his 60th birthday

0032-3861/90/101816-07

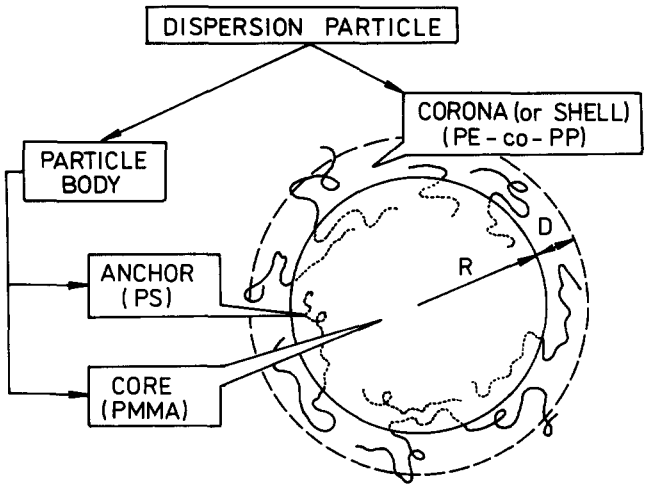

Figure 1 Sketch of a dispersion particle. The core consists of the dispersion polymer (PMMA), and the body of PMMA and anchor chains (the polystyrene block of the diblock copolymer steric stabilizer). The shell (or corona) is formed by the poly(ethylene-*co*-propylene) blocks of the diblock copolymer

in decane. The present results form part of a systematic study on the preparation of polymer dispersions. Here, we try to establish the methodology of characterization of dispersion particles: problems that can be encountered are pointed out, together with suggestions for their solution.

EXPERIMENTAL

Dispersion polymerization

A calculated amount of azo-*bis*-*iso*-butyronitrile (AIBN; purum, BDH, England) dissolved in methyl methacrylate (MMA; purum, Lachema, Czechoslovakia) was added to a decane (purum, Fluka, Switzerland) solution of the steric stabilizer, polystyrene-*block*-poly(ethylene-*co*-propylene) diblock, copolymer (Kraton G 1701, Shell; 42 wt% of styrene units, $M_w = 1.1 \times 10^5$ g mol^{-1}, $M_w/M_n \sim 1.1$). The concentration of the initiator, AIBN, was 1.0×10^{-3} g cm^{-3}. Mixtures were sealed under nitrogen into glass ampoules, and were allowed to polymerize at 60°C for 70 h (*Table 1*. Conversions of monomer over 98 wt% have been achieved. All the stabilizer was incorporated into the dispersion particles; after centrifugation, the supernatant liquid did not contain any polymer species.

Scanning electron microscopy (SEM)

Dispersions were diluted 1:2000 with decane, and a droplet of the solution on a brass support was quickly dried *in vacuo*. For SEM observation, the samples were coated with a layer of gold in an ion-sputtering device (Balzers 07120) at 13 Pa, 5 mA, target-to-sample distance 60 mm, sputtering time 3 × 3 min, with 5 min pauses. Micrographs were taken using a JSM 35 JEOL microscope at 25 kV, working distance 15 mm, magnification 40 000.

Refractive-index increments

The refractive-index increments v (cm^3 g^{-1}) of PMMA dispersions in decane ($\lambda_0 = 633$ nm, 25°C) were calculated according to the formula:

$$v = v_S x_S + v_P(1 - x_S) \quad (1)$$

where x_S is the mass fraction of the steric stabilizer in the dispersed particles (cf. *Table 1*). The refractive-index increment of the stabilizer, $v_S = 0.117$ cm^3 g^{-1}, was determined with a Brice–Phoenix differential refractometer BP-2000-V, while that of insoluble PMMA, $v_P = 0.078$ cm^3 g^{-1}, had to be estimated by interpolation of data available in the literature[11]. In two cases the calculated value for the dispersion was checked by direct measurement, because differential refractometry was not disturbed by the opalescence of the solution. The refractive-index increment of the polystyrene anchor block has been estimated from the simple additivity rule[1] as $v_A = 0.165$ cm^3 g^{-1}, and that of the shell chains as $v_C = 0.082$ cm^3 g^{-1}.

Static light scattering (SLS)

Dispersions were diluted 1:1000 (D3) or 1:2500 (D5,6,11) with decane, and further dilution was made to obtain a concentration series of solutions for measurement. Solutions were filtered through Uni-Pore polycarbonate membranes (Bio-Rad Laboratories, USA), porosity 0.6 μm. Light scattering was measured with a modified Sofica 42.000 apparatus using 7 mW He–Ne laser ($\lambda_0 = 633$ nm) as the light source. Some additional measurements were performed with a Chromatix KMX-6 low-angle laser light-scattering photometer. Attenuators were used to decrease the intensity of both the primary beam and the scattered light. With both types of equipment, virtually identical particle molar masses were obtained.

Dynamic light scattering (DLS)

A lab-made homodyne spectrometer was used in DLS measurements ($\lambda_0 = 633$ nm, $\theta = 45°$). The photopulse signal was analysed in a 96-channel digital correlator. The collective diffusion coefficients D_c of the dispersion particles were evaluated from the autocorrelation curves by a forced single-exponential fit. The hydrodynamic radius R_h was calculated from the Stokes–Einstein equation, $R_h = kT/(6\pi\eta D_c)$, where k is the Boltzmann constant and η (= 0.86 cP) is the viscosity of decane at 25°C. Owing to the high dilution of the dispersions, the concentration dependence of the diffusion coefficient was neglected. By assuming (a) the Pearson distribution of characteristic correlation times, (b) a spherical shape of the particles, and (c) a simple scaling law between the diffusion coefficient and molar mass of the particles ($D_c \sim M^{-1/3}$), non-uniformity expressed by the mass-to-number-average molar-mass ratio M_w/M_n was obtained[12].

Independent determinations of the diffusion coefficient were made on a Sofica 42.000 apparatus adapted for the

Table 1 Conditions for the dispersion polymerization of methyl methacrylate in decane. ϕ_M is the volume fraction of MMA in the reaction mixture; c_P and c_S are the concentrations of PMMA and of the steric stabilizer in the final dispersion; x_S is the mass fraction of the stabilizer in the dispersion particle

Dispersion	ϕ_M	$10^2 c_P$ (g cm^{-3})	$10^2 c_S$ (g cm^{-3})	x_S[a]
D3	0.10	8.80	1.5	0.145
D6	0.15	13.8	1.0	0.067
D5	0.15	13.8	0.5	0.035
D11	0.20	18.4	1.5	0.076

[a] Mass fractions of PMMA, $x_P = 1 - x_S$; of the shell (corona), $x_C = 0.58 x_S$; and of the anchor, $x_A = 0.42 x_S$

DLS measurements. Particle dimensions and their non-uniformity were further checked with a Coulter Nano-Sizer, which works on the DLS principle. All devices yielded virtually identical hydrodynamic radii.

RESULTS AND DISCUSSION

Electron microscopy

Scanning electron microscopy (SEM) was used to establish the spherical shape of PMMA particles formed in dispersion polymerization (*Figure 2*). A certain non-uniformity in particle dimensions can be noted. In the case of dispersion D11, a bimodal distribution of particle dimensions is suspected (*Figure 2d*), which is consistent with the high value of the M_w/M_n ratio (*Table 2*). The estimated average radius R_m of the particles (*Table 2*) includes the gold layer used in the preparation of the samples; the actual polymer particle size is correspondingly smaller. A comparison with the dimensions obtained by other methods is discussed below.

Evaluation of the static light-scattering data

The mass-average molar mass M_w of the dispersed particles can be evaluated from the static light-scattering measurement[1] after extrapolation of the data to zero polymer concentration c:

$$\lim_{c\to 0} \frac{Kc}{R_\theta} = \frac{1}{M_w P(\theta)} \tag{2}$$

and to zero angle θ. Here K is the optical constant, which includes the refractive-index increment, and R_θ is the Rayleigh ratio. The particle scattering function $P(\theta)$ depends on the shape and uniformity of the macro-

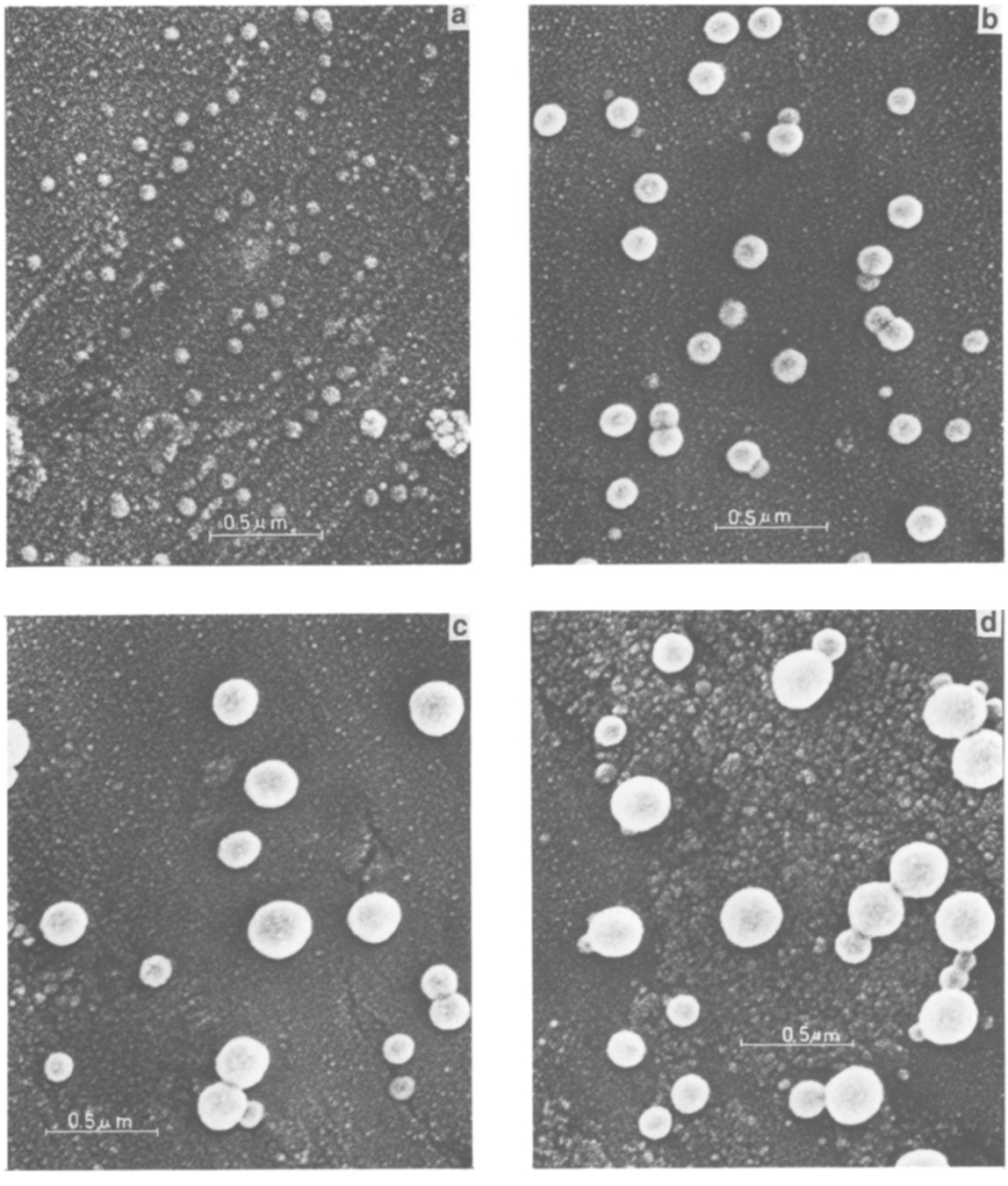

Figure 2 SEM micrographs of the dispersion particles: (a) D3, (b) D6, (c) D5 and (d) D11

Table 2 Mass-average particle molar mass M_w, mass- to number-average molar-mass ratio M_w/M_n, apparent radius of gyration s_{app}, hydrodynamic radius R_h and radius of dispersion particles R_m from SEM

Dispersion	$10^{-6}M_w$ (g mol^{-1}) [SLS]	M_w/M_n [DLS]	s_{app} (nm) [SLS]	R_h (nm) [DLS]	R_m (nm) [SEM]
D3	110	1.28	40	65	35
D6	1340	1.29	69	121	75
D5	4380	1.61	107	151	120
D11	6530	1.89	137	180	125

molecules or particles. Its initial slope is determined by the radius of gyration s (z-average in the case of non-uniform particles):

$$P^{-1}(\theta)=1+\tfrac{1}{3}q^2s^2+\cdots \quad (3)$$

where q is the length of the scattering vector:

$$q=(4\pi/\lambda)\sin(\theta/2) \quad (4)$$

and λ ($=\lambda_0/n$) and λ_0 are the wavelengths of light in a medium of refractive index n and *in vacuo*, respectively.

When the angular dependences in a Zimm plot are curved upwards, which is typical of large homogeneous spheres, the use of the logarithmic version of the Zimm plot has been recommended[5,6]; here, the ordinate is $\ln(Kc/R_\theta)$. From equation (2), we have:

$$\lim_{c\to 0}\ln\frac{Kc}{R_\theta}=\ln\frac{1}{M_w}+\ln\frac{1}{P(\theta)} \quad (5)$$

The values of the derivatives of $P^{-1}(\theta)$ and $\ln P^{-1}(\theta)$ with respect to $\sin^2(\theta/2)$ are identical at $\theta=0$:

$$\frac{\mathrm{d}\ln P^{-1}(\theta)}{\mathrm{d}\sin^2(\theta/2)}=P(\theta)\frac{\mathrm{d}P^{-1}(\theta)}{\mathrm{d}\sin^2(\theta/2)}=\frac{16\pi^2}{3\lambda^2}s^2 \quad (6)$$

since $P(0)=1$. This allows the radius of gyration to be determined in the same manner in both versions of the Zimm plot.

For uniform homogeneous spheres[1]:

$$P(\theta)=[3(\sin X-X\cos X)/X^3]^2 \quad (7)$$

where $X=qR=(5/3)^{1/2}qs$, R being the radius of the sphere. The efficiency of the curvature-suppressing procedure for the treatment of SLS data, outlined above, is shown in *Figure 3*, where the reciprocal particle scattering function of uniform homogeneous spheres, $P^{-1}(\theta)$, and its natural logarithm are plotted against q^2s^2 (in practice, usually against $\sin^2(\theta/2)$). Unity was added to the latter function to set the common origin for both functions at $\theta=0$. The function $P^{-1}(\theta)$ quickly deviates from the initial linear dependence with a slope of 1/3. Deviations of 5% and 10% are found for $q^2s^2=0.94$ and 1.39, respectively. For $\lambda_0=633$ nm and refractive index $n=1.412$ (decane), a nearly linear dependence is observed over the whole range of angles $\theta=0$ to 180° for spheres with $s<40$ nm. By a 'nearly linear' dependence we mean that the initial section of the curve does not deviate by more than 10% from the linear dependence with a slope of 1/3. Analogous values for the logarithmic plot are shifted to higher values of q^2s^2 (*Figure 3*); deviations of 5% and 10% are obtained for $q^2s^2=3.33$ and 4.98, respectively, and the nearly linear angular dependences occur for spheres with $s<80$ nm. If the requirement of near-linearity is restricted to angles $\theta<90°$, which is sufficient for the majority of practical particle-mass determinations, the limiting value of the radius of gyration can be set to about $80\times(2)^{1/2}=113$ nm. For homogeneous uniform spheres, this corresponds to a geometric radius of $113\times(5/3)^{1/2}=146$ nm.

This prediction, based on model calculations, has been confronted with the experimental data (*Table 2, Figure 4*). Both the conventional and logarithmic versions of the Zimm plot[1] show linear angular dependences if the dispersion particles are small (*Figure 4a*, D3, $s=40$ nm). For larger particles, the dependences in the conventional plot have an upward curvature, typical of uniform spheres (*Figure 4b*, D6, $s=69$ nm), which is readily linearized in the logarithmic modification. In both plots, extrapolation to zero angle can still be made without difficulty, and the same particle molar mass is obtained. However, the determination of the radius of gyration is considerably more precise in the logarithmic plot.

The conventional plot of the light-scattering data for still larger particles (*Figure 4c*, D5, $s=107$ nm) cannot be used to derive either the particle molar mass or the radius of gyration with tolerable accuracy; both quantities are easily evaluated from the logarithmic plot.

Finally, the largest particles that were characterized (*Figure 4d*, D11, $s=137$ nm) give rise to a slightly sigmoidal conventional plot and, consequently, the logarithmic modification is curved in the region of large angles. The function $P^{-1}(\theta)$ for uniform spheres has its first maximum at $\theta=180°$ for the particle radius $R=160.5$ nm (for $\lambda_0=633$ nm, $n=1.412$), which corresponds to a radius of gyration $s=124.3$ nm. For dispersion D11, which has a larger radius of gyration, a maximum on the angular dependences can thus be expected to occur at angles $\theta<180°$. Owing to the non-uniformity of the particles, the maximum is smeared, and manifests itself only as a downward curvature at large angles.

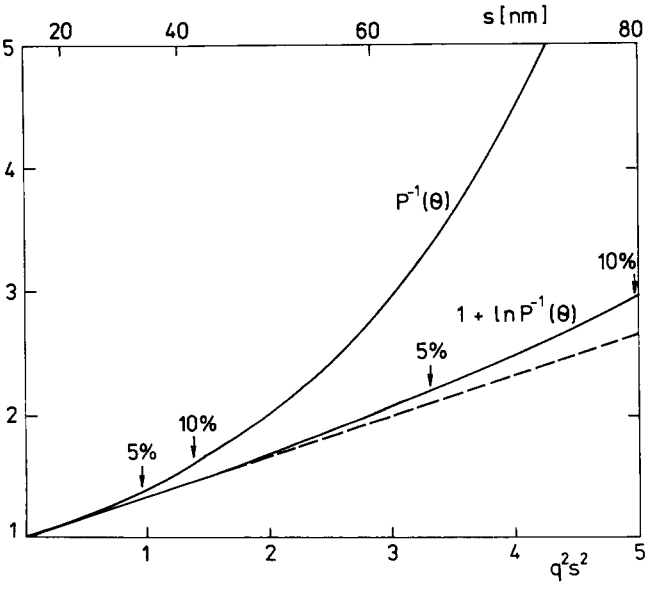

Figure 3 The reciprocal particle scattering function $P(\theta)^{-1}$ for uniform homogeneous spheres and its logarithm $\ln P(\theta)^{-1}$ as a function of q^2s^2. The length of the scattering vector q is given by equation (4). The upper scale is labelled by the radii of gyration s for which q^2s^2 assumes the given value at $\theta=180°$, for $\lambda_0=633$ nm and $n=1.412$. The broken straight line has a slope equal to 1/3, which is the initial slope of any reciprocal particle scattering function dependence on q^2s^2

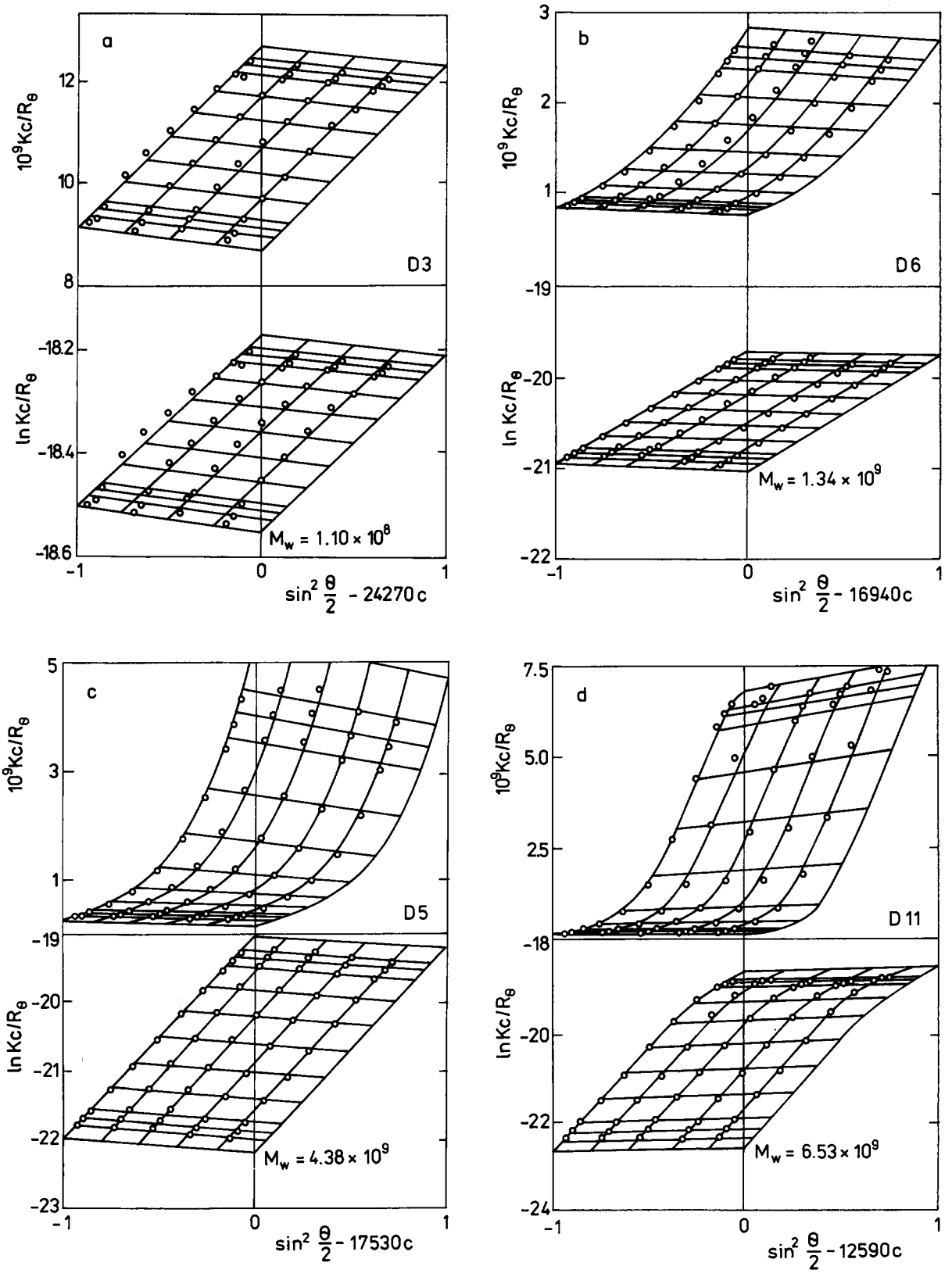

Figure 4 Classical and logarithmic versions of the Zimm plot for PMMA dispersions in decane: (a) D3, (b) D6, (c) D5 and (d) D11

Particle dimensions

The apparent radius of gyration s_{app} (the quantity obtained from SLS for the present, non-homogeneous dispersion particles) includes[13] contributions from the polymer core, the anchor and the shell (corona):

$$s_{app}^2 = \sum_i \frac{v_i}{v} x_i s_i^2 \qquad (8)$$

where the subscripts $i = P$, A and C refer to the individual particle parts. Equation (8) holds for particles, all parts of which have a common centre of mass. We assume that the polymer core is a homogeneous sphere with a geometric radius R, in which the anchor chains form, to a first approximation, a surface layer over the polymer core with negligible thickness (i.e. a hollow sphere of

radius R), and the shell has a thickness of D (i.e. it can be regarded as a hollow sphere of radius $R+D$ with a cavity of radius R) (*Figure 1*). For such structures[14]:

$$s^2_{app}=0.6\frac{v_P x_P}{v}R^2+\frac{v_A x_A}{v}R^2+0.6\frac{v_C x_C}{v}\frac{(R+D)^5-R^5}{(R+D)^3-R^3} \quad (9)$$

Owing to the high mass fraction x_P of the polymer in a particle, the first term of equation (9) dominates the whole sum, but the remaining two terms have to be considered in a detailed analysis. It has been shown that the shell thickness D is comparable with or slightly higher than the mean end-to-end distance of a homopolymer corresponding to shell chains[15,16]. For a poly(ethylene-*co*-propylene) block of molar mass $M_S=58\,000$ g mol^{-1}, this dimension could be estimated, based on literature data[17], as $D=26$ nm. The value of the radius R is then sought by numerical computer calculation, which makes the right-hand side of equation (9) equal to the apparent radius of gyration determined experimentally (*Table 3*).

Assuming that the anchor chains are homogeneously distributed throughout the particle core, and are not located on its surface only, the second right-hand term in equation (9) has also to be multiplied by the factor 0.6. Values of R higher by 1–3% are obtained, as compared to the previous case. Thus the two models cannot be distinguished by the present experimental method. Complete neglect of the shell, i.e. the assumption that $s^2_{app}=0.6R^2$, leads to an overestimation of the geometric radius of the core (*Table 3*), especially with small particles, where the mass fraction of the shell is relatively large (*Table 1*).

Particle swelling

For the following discussion, it is useful to distinguish between the particle core, consisting of PMMA, and the particle body, which includes also the anchor chains. The particle body thus consists of insoluble components while the shell is composed of soluble chains. In our considerations, both the core and the body have identical geometric radii R, but they differ somewhat in molar mass, by definition. In our opinion, it is more rigorous to consider the swelling of the particle body rather than that of its core.

Once the radius R of the body is known, the degree of swelling of the body defined by the ratio $\Phi=V/V_d$ of the volumes of the swollen and dry entities, respectively, can be calculated. The volume of a dry body is $V_d=(1-x_C)M/\rho N_A$, where ρ is the polymer density ($\rho=1.19$ g cm^{-3} for a PMMA core[18], and this value can also be used for PMMA containing a few per cent of the polystyrene anchor blocks). The factor $(1-x_C)$ converts the molar mass M of the whole particle to that of the particle body and N_A is the Avogadro constant. Hence:

$$\Phi=\frac{4\pi\rho N_A R^3}{3(1-x_C)M} \quad (10)$$

The volume fraction of the dispersion medium in the body is related by $\phi=1-\Phi^{-1}$ (*Table 3*).

Equation (10) holds exactly only for uniform spheres. In non-uniform systems, the z-average radius of gyration $\langle s^2\rangle_z$ and the mass-average molar mass M_w are obtained from SLS. For particles with complex internal structures, such as the dispersion particles under consideration, the value of the radius R of the body satisfying equation (9) may not be exactly the z-average of this quantity. However, to estimate the effect of non-uniformity on the calculated degree of swelling, it seems to be admissible—owing to the dominating role of the first term in equation (9)—to identify the computed value of R with the true z-average value. The use of the different averages in equation (10) overestimates the degree of swelling, like the neglect of the shell in the estimation of the core radius. The molar mass M_s of homogeneous uniform spheres that have the squared radius of gyration s^2 equal to $\langle s^2\rangle_z$ of an assembly of non-uniform spheres with the differential mass distribution function of molar masses $W(M)$ is given by[19]:

$$M_s=\frac{1}{M_w}\left(\int_M M^{4/3}W(M)\,dM\right)^{3/2} \quad (11)$$

So far, the type of molar-mass distribution displayed by the dispersion particles has not been established persuasively in the literature. Assuming that $W(M)$ of the Schulz–Zimm type is appropriate[20] for particle dispersions:

$$W(M)=\frac{b^{a+1}}{\Gamma(a+1)}M^a\exp(-bM) \quad (12)$$

where $a=[(M_w/M_n)-1]^{-1}$ and $b=(a+1)/M_w$, we can write:

$$\frac{M_s}{M_w}=\frac{1}{a+1}\left(\frac{\Gamma(a+\frac{8}{3})}{\Gamma(a+2)}\right)^{3/2} \quad (13)$$

$\Gamma(m)$ is the gamma function of argument m. The dependence of M_s/M_w on M_w/M_n is shown in *Figure 5*.

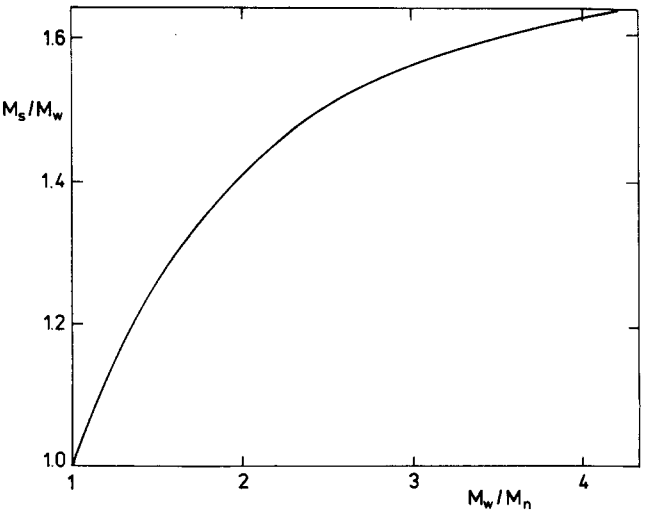

Figure 5 The dependence of M_s/M_w for spherical particles on M_w/M_n according to equation (13)

Table 3 Geometric radii of the particle body R, the corresponding swelling ratio Φ and the volume fraction of the solvent ϕ in particle body

	The effect of shell and of particle non-uniformity					
	is neglected			is considered		
Dispersion	R	Φ	ϕ	R	Φ	ϕ
D3	52	3.83	0.74	46	2.50	0.60
D6	89	1.59	0.37	85	1.23	0.19
D5	138	1.80	0.44	136	1.35	0.26
D11	176	2.51	0.60	170	1.71	0.42

The use of the corrections for the effect of the shell and of particle non-uniformity reduces the swelling ratio Φ by about 30%. Generally, the content of the dispersion medium in the particle body seems to be rather large, so that most of the particles are to be regarded as highly swollen (*Table 3*).

Particle size determined by other methods

Dynamic light scattering can be used to determine the hydrodynamic radii R_h of the particles. Unlike SLS, where the measured dimensions are determined mainly by the particle body, in DLS the shell affects the hydrodynamic (diffusion) behaviour of the dispersion particle, and the hydrodynamic radii should generally be larger than the radii of the body, $R_h > R$. This is indeed the case (*Table 2*), and the difference $R_h - R = (20 \pm 9)$ nm is in tolerable agreement with the assumed shell thickness, $D = 26$ nm, estimated from the end-to-end distance of poly(ethylene-*co*-propylene) chains[17] (cf. *Figure 1*).

The radii R_m estimated from SEM (*Table 2*) correspond to dry particles, i.e. they are smaller compared to the dimensions of swollen particles, $R_m < R$. Since we know the swelling ratio Φ (*Table 3*), the radius of the dry particle can be calculated, $R_d = R/\Phi^{1/3}$. On average, $R_d - R_m = (6 \pm 4)$ nm. However, the thickness of the gold layer applied in the preparation of the samples for SEM is not precisely known and any further quantitative discussion would be speculative. The SEM has primarily been used to establish the shape and the degree of uniformity of the particles.

CONCLUSIONS

Light scattering is a powerful tool for the characterization of dispersion particles in the submicrometre range. SLS allows the particle molar mass to be determined directly, along with the radius of gyration. DLS provides the hydrodynamic radius of the particle and information on non-uniformity of the particles. These quantities can be combined to estimate the extent of particle swelling, an important characteristic difficult to obtain by other techniques.

REFERENCES

1 Kratochvíl, P. 'Classical Light Scattering from Polymer Solutions', Polymer Science Library, Vol. 5 (Ed. A. D. Jenkins), Elsevier, Amsterdam, 1987
2 Tuzar, Z. and Kratochvíl, P. *Adv. Colloid Interface Sci.* 1976, **6**, 201
3 Price, C., Kendall, K. D., Stubbersfield, R. B. and Wright, B. *Polym. Commun.* 1983, **24**, 200
4 Stejskal, J., Straková, D. and Kratochvíl, P. *J. Appl. Polym. Sci.* 1988, **36**, 215
5 Wesslau, H. *Makromol. Chem.* 1963, **69**, 220
6 Burchard, W., Keppler, D. and Decker, K. *Makromol. Chem.* 1968, **115**, 250
7 'Dispersion Polymerization in Organic Media' (Ed. K. E. J. Barrett), Wiley, London, 1975
8 Winnik, M. A., Lukas, R., Chen, W. F., Furlong, P. and Croucher, M. D. *Makromol Chem., Macromol. Symp.* 1987, **10/11**, 483
9 Dawkins, J. V. and Taylor, G. *Colloid Polym. Sci.* 1980, **258**, 79
10 Barrett, K. E. J. and Thomas, H. R. *J. Polym. Sci. (A-1)* 1969, **7**, 2621
11 Ochiai, H., Kamata, K. and Murakami, I. *Polym. Commun.* 1984, **25**, 158
12 Jakěs, J. '3rd International Symposium on Polymer Analysis and Characterization', Brno, Czechoslovakia, 1990
13 Benoît, H. and Froelich, D. in 'Light Scattering from Polymer Solutions' (Ed. M. B. Huglin), Academic Press, London, 1972, p. 484
14 Tuzar, Z., Pleštil, J., Koňák, Č., Hlavatá, D. and Sikora, A. *Makromol. Chem.* 1983, **284**, 2111
15 Candau, F., Heatley, F., Price, C. and Stubbersfield, R. B. *Eur. Polym. J.* 1984, **20**, 685
16 Rigby, D. and Roe, R.-J. *Macromolecules* 1986, **19**, 721
17 'Polymer Handbook' (Eds. J. Brandrup and E. H. Immergut), 2nd Edn., Wiley Interscience, New York, 1974, pp. iv, 35–6
18 Sewell, J. H. *J. Appl. Polym. Sci.* 1973, **17**, 1741
19 Kratochvíl, P. in 'Light Scattering from Polymer Solutions' (Ed. M. B. Huglin), Academic Press, London, 1972, p. 345
20 Maxim, L. D., Klein, A., Meyer, M. E. and Kuist, C. H. *J. Polym. Sci. (C)* 1969, **27**, 195